# Structure, Microtubule Interactions, and Paired Helical Filament Aggregation by Tau Mutants of Frontotemporal Dementias †

**ARTICLE** *in* BIOCHEMISTRY · OCTOBER 2000

Impact Factor: 3.02 · DOI: 10.1021/bi000850r · Source: PubMed



**6 AUTHORS**, INCLUDING:

Stefan Barghorn
AbbVie
**24** PUBLICATIONS **1,805** CITATIONS
SEE PROFILE

Martin Von Bergen
Helmholtz-Zentrum für Umweltforschung
**246** PUBLICATIONS **6,021** CITATIONS
SEE PROFILE

# Structure, Microtubule Interactions, and Paired Helical Filament Aggregation by Tau Mutants of Frontotemporal Dementias[†]

S. Barghorn, Q. Zheng-Fischhöfer, M. Ackmann, J. Biernat, M. von Bergen, E.-M. Mandelkow, and E. Mandelkow*

*Max-Planck-Unit for Structural Molecular Biology, c/o DESY, Notkestrasse 85, D-22607 Hamburg, Germany*

*Received April 14, 2000; Revised Manuscript Received July 3, 2000*

ABSTRACT: We have studied biochemical and structural parameters of several missense and deletion mutants of tau protein (G272V, N279K, ΔK280, P301L, V337M, R406W) found in frontotemporal dementia and parkinsonism linked to chromosome 17 (FTDP-17). The mutant proteins were expressed on the basis of both full-length tau (htau40) and constructs derived from the repeat domain. They were analyzed with respect to the capacity to enhance microtubule assembly, binding of tau to microtubules, secondary structure content, and aggregation into Alzheimer-like paired helical or straight filaments. We find that the mutations cause a moderate decrease in microtubule interactions and stabilization, and they show no gross structural changes compared with the natively unfolded conformation of the wild-type protein, but the aggregation into PHFs is strongly enhanced, particularly for the mutants ΔK280 and P301L. This gain of pathological aggregation would be consistent with the autosomal dominant nature of the disease.

Alzheimer's disease is characterized by abnormally aggregated proteins, composed largely of the A$\beta$ peptide in the case of amyloid plaques, and of tau protein in the case of neurofibrillary tangles and related deposits. Tau is a microtubule-associated protein that is thought to stabilize axonal microtubules and support neurite outgrowth [see review in (*1*, *2*)]. It is normally highly soluble, but in Alzheimer's disease it aggregates into fibers, mostly "paired helical filaments" (PHFs),[1] which further coalesce into neurofibrillary tangles (NFTs). The pathway of spreading of tau deposits throughout the brain cortex forms the basis of subdividing the disease into 6 stages (*3*) and correlates with the degree of neuronal loss (*4*, *5*). Similar deposits can occur in other neurodegenerative diseases as well [e.g., progressive supranuclear palsy, corticobasal degeneration, and frontotemporal dementias; see review in (*6*, *7*)], although they appear less numerous and have a different distribution. A fraction of Alzheimer's disease cases correlate with defects in one of several genes [e.g., APP, PS-1, PS-2; see review in (*8*)], but no mutation was reported for the *tau* gene on chromosome 17. However, it was discovered recently that a group of frontotemporal dementias collectively termed FTDP-17 (*9*) were related to mutations in tau. These dementias showed neurofibrillary deposits similar to Alzheimer's disease which therefore opened a possibility to study the mechanisms underlying both Alzheimer's disease and related tauopathies. Some mutations were missense mutations, e.g., G272V (*10*), N279K (*11*), P301L or P301S (*12*), S305N (*13*), V337M (*12*), or R406W (*10*). There was one deletion mutant ΔK280 (*14*), one silent mutation L284L (*15*), and several intronic mutations which affect the stability of a stem loop structure following exon 10 (*10*, *15*−*18*). All mutations occurred in or near the microtubule-binding domain of tau which consists of the repeats and flanking regions (*19*−*21*) (see Figure 1). This argues that mutant tau protein may be deficient in its capacity to regulate the stability of neuronal microtubules. In principle, this could take the form of over- or understabilization, both of which would perturb the physiological process of dynamic instability (*22*); analogous defects are known for certain anticancer drugs which work either by stabilizing microtubules (e.g., taxol) or by disrupting them [e.g., vinblastine; see review in (*23*)].

The repeat domain of tau and its adjacent regions not only are involved in the binding of tau to microtubules, but also are involved in the tau−tau interactions that lead to the pathological aggregation of PHFs. The repeats are found in the protease-resistant core of Alzheimer PHFs (*24*, *25*), and aggregation of tau into PHFs in vitro is most efficient with constructs encompassing the repeat domain (*26*−*30*). Thus, a second pathological role of the tau mutations could be to speed up the process of aggregation. Both effects—microtubule binding and PHF aggregation—have been investigated by several authors. It appears that certain tau mutations tend to weaken tau's capacity to bind to microtubules (*15*, *31*, *32*), lower its support of the assembly of microtubules (*15*, *31*, *33*−*36*), and enhance PHF aggregation (*37*−*40*), although there is disagreement on the magnitude of the effects and the relative efficiencies of the different mutants.

We have recently developed an assay based on the fluorescence of the dye thioflavine S that enables us to quantify the rate and extent of PHF aggregation in vitro (*41*). We have now used this assay to determine the aggregation of tau constructs and mutants. Six of the missense or deletion mutants have been generated on the basis of full-length tau

[†]This work was supported by the Deutsche Forschungsgemeinschaft.

* Corresponding author. Tel: +49-40-89982810, Fax: +49-40-89716822, e-mail: mand@mpasmb.desy.de.

[1] Abbreviations: AD, Alzheimer's disease; FTDP-17, frontotemporal dementia and parkinsonism linked to chromosome 17; NFTs, neurofibrillary tangles; PHF, paired helical filament.

10.1021/bi000850r CCC: $19.00 
Published on Web 09/01/2000

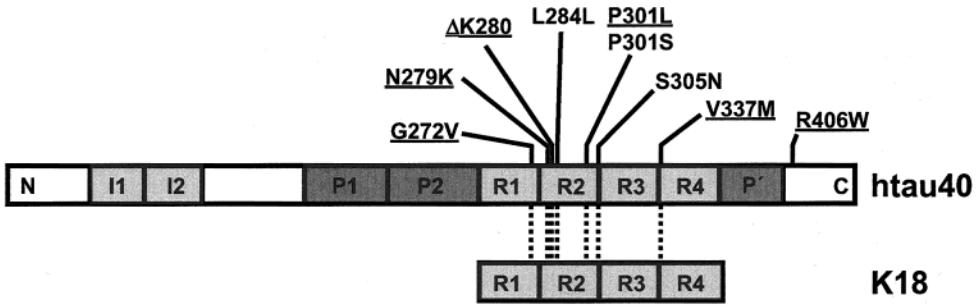


FIGURE 1: Diagram of FTDP-17 mutations in tau and the construct K18. The upper bar shows htau40, the largest isoform in the human CNS (441 residues). The C-terminal half contains 3 or 4 pseudo-repeats (~31 residues each, R1−R4) which together with their flanking regions (proline-rich, dark shade) constitute the microtubule-binding domain. Repeat R2 and the two near-N-terminal inserts (I1, I2) may be absent due to alternative splicing. The known FTDP-17 mutations are concentrated in the microtubule-binding domain. Mutations N279K, ΔK280, P301L, and P301S are located in R2 and thus affect only 4-repeat isoforms of tau; the others shown here occur in all tau isoforms. Further mutations (not shown) occur in noncoding regions of the *tau* gene following exon 10 (corresponding to R2). Construct K18 comprises only the 4 repeats and has been generated with the corresponding mutations (dotted lines). Mutations investigated in this study are underlined.

(htau40 isoform, containing 4 repeats) and on the basis of construct K18 which consists of the 4 repeats only. We find that all mutants have a similar mostly random-coil structure in solution and show only moderate differences in their microtubule-assembling activities, but can have dramatically enhanced tendencies for aggregation, especially ΔK280 and P301L mutants. In all cases, electron microscopy shows filaments resembling the paired helical and straight filaments of Alzheimer tau.

## MATERIALS AND METHODS

*Chemicals and Proteins.* Taxol, heparin (average MW of 6000), and thioflavine S were obtained from Sigma (Steinheim, Germany). Human tau40 and construct K18 (see Figure 1) were expressed in *E. coli* as described (*42*). The numbering of the amino acids is that of the isoform htau40 containing 441 residues (*43*). The protein was expressed and purified as described elsewhere (*20*), making use of the heat stability and FPLC Mono S chromatography with subsequent gel-filtration [Superdex 200 for htau40 and Superdex 75 for the construct K18 (Amersham Pharmacia Biotech, Freiburg, Germany)]. The purity of the proteins was analyzed by SDS−PAGE. Protein concentrations were determined by Bradford assay or by UV absorption at 214 nm. The mutations of htau40 and construct K18 were created by site-directed mutagenesis which was performed using the Quick-change kit (Stratagene, Amsterdam, The Netherlands) and the plasmid pNG2-K18 (*20*). Plasmids were sequenced on both strands.

*PHF Assembly.* Aggregation was induced by incubating varying concentrations of tau isoforms or tau constructs (typically in the range of 10−50 μM) in volumes of 20−500 μL at 37 °C in PBS, pH 7.4, containing 1−10 mM DTT and anionic cofactor heparin (*41*). Preparations of htau40 were supplemented with protease inhibitor mix containing 1 mM PMSF, 1 mM EDTA, 1 mM EGTA, 1 μg/mL leupeptin, 1 μg/mL aprotinin, and 1 μg/mL pepstatin. Prior to incubation and heparin addition, samples were heated for 5 min at 50 °C to ensure complete reduction of tau to monomers. Incubation times varied from minutes up to several days. The formation of aggregates was ascertained by ThS fluorescence and electron microscopy.

*Fluorescence Spectroscopy.* Fluorescence was measured with a Fluoroskan Ascent spectrofluorometer (Labsytems, Helsinki, Finland) with an excitation filter of 480 ± 5 nm and an emission filter of 510 ± 5 nm in a 384 well plate. Measurements were carried out at room temperature in PBS, pH 7.4, with 10 μM ThS unless otherwise stated. Background fluorescence and light scattering of the sample without thioflavine S were subtracted when needed.

*Electron Microscopy.* Protein solutions diluted to 1−10 μM protein were placed on 600-mesh carbon-coated copper grids for 45 s, washed twice with $H_2O$, and negatively stained with 2% uranyl acetate for 45 s. The specimens were examined with a Philips CM12 electron microscope at 100 kV.

*Circular Dichroism Spectroscopy.* All measurements were made with a Jasco J-710 CD-Dichrograph (Jasco, Tokio, Japan) in a cuvette with 0.05 cm path length. In each experiment, equimolar concentrations were used, and 10 spectra were summed up to determine the molar ellipticity. The secondary structure interpretation of the CD data was performed according to Greenfield and Fasman (*44*), as implemented in the program Dicroprot (*45*).

*Light Scattering.* Microtubule assembly was monitored by light scattering at 90° and 350 nm wavelength on a Kontron spectrophotometer (*46*); 5 μM tau was mixed with 30 μM tubulin dimer at 4 °C. The reaction was started by raising the temperature to 37 °C with defined heating rates. Turbidity was measured in a quartz cuvette (10 mm path length). Three parameters were extracted from the curves: the maximum turbidity at steady state, the rate of assembly, and the lag time between the temperature jump and the start of the turbidity rise. Three experiments were performed for each tau mutant.

*Microtubule Binding Assay.* The MT binding assay was performed as described (*47*). Briefly, a fixed MT concentration was incubated for 20 min at 37 °C with varying concentrations of tau. The suspension was fractionated by centrifugation for 8 min at 62000*g* at 25 °C. Tau in the supernatant (tau free) and the pellet (tau bound) was determined by an ELISA. The data were interpreted in terms of biphasic binding behavior. Bound tau was plotted versus free tau and fitted against the equation:

$$[\text{tau}]_{\text{bound}} = \frac{n \cdot [\text{MT}] \cdot [\text{tau}]_{\text{free}}}{K_d + [\text{tau}]_{\text{free}}} + \frac{1}{p} \cdot [\text{MT}] \cdot [\text{tau}]_{\text{free}}$$

where the first term (dominating at low tau concentrations) describes equivalent and noninteracting binding sites with a

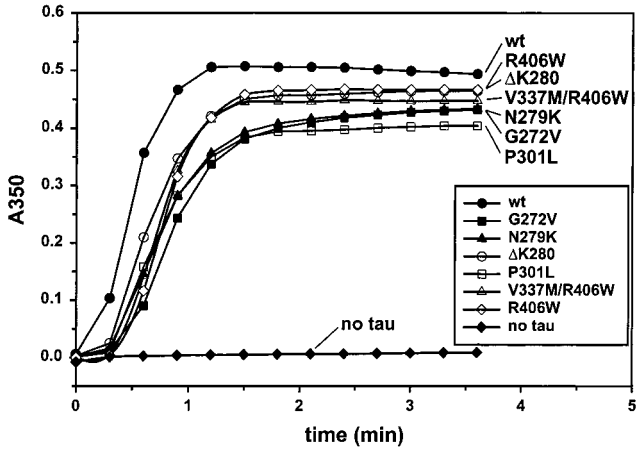


FIGURE 2: Microtubule assembly promoted by htau40 and its mutants. Assembly of microtubules is observed by the optical density at 350 nm ($A_{350}$). 30 $\mu$M tubulin (dimer concentration) was mixed with 5 $\mu$M tau at 4 °C. The reaction was started by warming up the samples to 37 °C. Tubulin alone is unable to polymerize because its concentration is below the critical concentration (bottom curve). Wild-type htau40 induces assembly with a half-time of ~20 s and a lag time of ~5 s. All htau40 mutants show a similar slightly decreased ability to promote MT assembly (half-time ~40 s, lag time ~20 s). One representative experiment is shown for each mutant; similar results were obtained in three separate experiments (reproducibility ~5%).

dissociation constant $K_d$ and a stoichiometry of $n$ tau molecules per tubulin subunits, and the second term describes a weak and nonsaturable binding at higher tau concentrations with an "overloading parameter" $p$. It describes the fact that tau tends to accumulate on the microtubule surface in a nonstoichiometric manner [for details, see (*47*)].

## RESULTS

*(a) Tau Mutants Have a Reduced Ability To Promote MT Assembly.* To determine the effect of the missense mutations on specific functions of tau, we first investigated the ability of tau to promote MT assembly by using the light scattering method. The conditions were similar to those used previously to study the effects of tau domains (*20*). The tubulin concentration (30 $\mu$M) was below the critical concentration of the protein so that almost no turbidity increase was observed without tau. With 5 $\mu$M htau40$^{wt}$, the scattering increased rapidly and reached maximal turbidity within 1 min, illustrating the strong assembly-promoting effect of tau (Figure 2). Typical half-times were ~20 s, and the lag time necessary for microtubule nucleation was very short (a few seconds). The experiments were reproducible within <5% with samples from the same protein batch. When the mutants of htau40 were tested with the same procedure, they all showed a lower ability to promote microtubule assembly. The lag times became longer (~20 s), the same was true for half-maximal assembly times (~40 s), and the extent of assembly decreased by 10−20%. Although some differences between mutants were observed, they were not significant (~10% variation in half-times and maximal levels), and faster assembly did not imply a higher degree of assembly. In particular, we note that the assembly rate depends on a combination of nucleation efficiency, elongation rate, and parameters of dynamic instability which cannot be observed separately in this type of experiment; nevertheless, the reproducibility of measurements and the close agreement between the different mutants are notable.

*(b) The Binding of Tau Mutants to Taxol-Stabilized Microtubules Varies Considerably.* We next evaluated the binding properties of htau40$^{wt}$ and mutants to taxol-stabilized MTs. Different tau concentrations were incubated with a constant MT concentration of 3 $\mu$M (tubulin dimer = effective polymerizing subunit). MT-bound and -unbound tau fractions were separated by centrifugation, and the tau concentration was determined by a sandwich-ELISA (*47*). Bound tau was plotted versus free tau and fitted against a biphasic binding equation (see Materials and Methods). The "tight binding" phase is observed only at low tau concentrations since a more detailed analysis showed a second nonsaturable low-affinity binding phase which became noticeable at higher tau concentrations and can be described by the "overloading parameter" $p$. The effect partly explains the discrepancies between reported dissociation constants and will be described in more detail elsewhere (*47*). As shown in Figure 3 and Table 1, htau40$^{wt}$ binds tightly with a first phase $K_d$ of 0.075 $\mu$M and a stoichiometry of 0.20. Using the stoichiometry of the tight binding phase as a basis for classification, we can distinguish three groups (Table 1): The medium group includes htau40$^{wt}$ and the mutants G272V, V337M, and R406W which have stoichiometries around 0.2−0.3, first-phase $K_d$ values below 0.1 $\mu$M, and "overloading parameters" $p$ around 40−50 $\mu$M (these can be considered roughly as $K_d$ values of the second "loose" binding phase). The high group includes ΔK280 and P301L because they decorate microtubules with a higher stoichiometry (around 0.4), without much change in the other parameters. N279K is a group by itself; it shows very little tight binding (low stoichiometry of 0.07) and a low $p$-value so that binding becomes noticeable only at high concentrations. Summarizing these results, it appears that the influence of tau mutations on microtubule binding is more heterogeneous than on microtubule assembly so that the two quantities are not correlated in an obvious fashion. We note that mutants ΔK280 and P301L show a higher stoichiometry than the rest, which correlates with their PHF aggregation (see below).

*(c) Tau Mutations Cause No Gross Change in the Overall Random Coil Secondary Structure.* To assess the secondary structure of tau mutants in solution, we measured their CD spectra. Earlier studies had revealed a mostly random coil conformation of tau (*48*), and this was confirmed here (Figure 4). All spectra show a minimum around 200 nm which is characteristic of random coil, and there was no evidence for appreciable α-helical or $\beta$-sheet secondary structure components (Figure 4). The depths of the minima at 200 nm are variable; the lowest one is observed for R406W; an intermediate group comprises htau40$^{wt}$, V337M, and P301L; and the shallowest minimum is seen with the group of G272V, N279K, and ΔK280. As noted before, there is no obvious correlation between the CD spectra of Figure 4 and microtubule assembly stimulation (Figure 2) or microtubule binding (Figure 3). Apart from that, the variation between the spectra does not provide a significant indicator for differences in secondary structure since the reference spectra used in common algorithms (*49*) are not reliable for structures dominated by random coil. We therefore conclude that the mutations do not change tau's structure in a quantifiable manner.

*(d) Filament Formation Is Accelerated in Tau Mutants.* Next we asked whether the mutations in tau would alter their

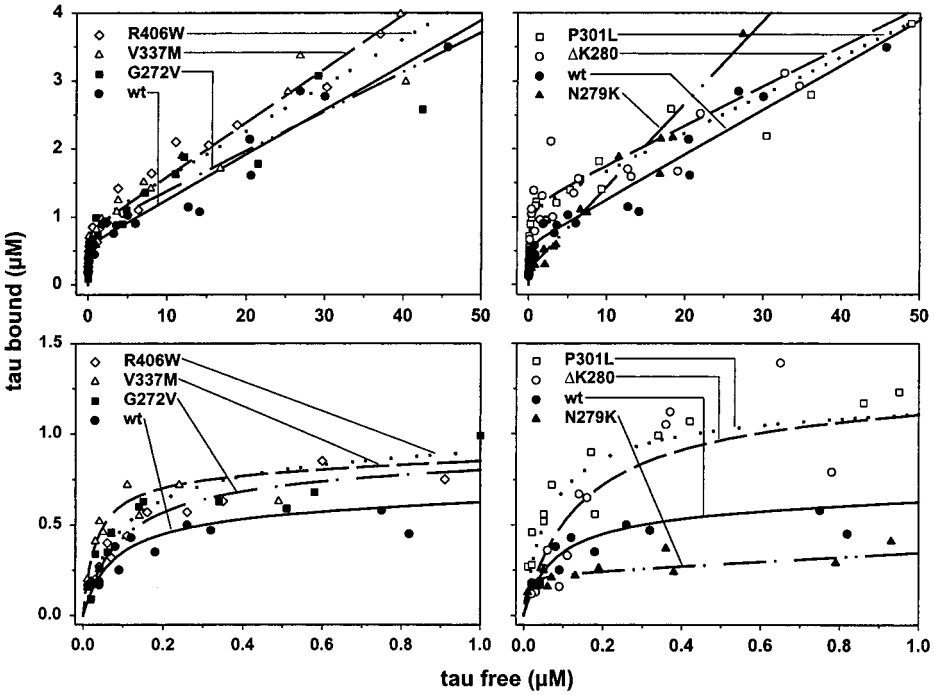


FIGURE 3: Microtubule binding of htau40$^{wt}$ and mutants. Tubulin was polymerized into microtubules and stabilized by taxol. Different tau concentrations were incubated with 3 $\mu$M microtubules, bound and free fractions were separated by sedimentation, determined by the tau ELISA, and the plot of bound tau versus free tau was fitted against a biphasic binding equation (see Materials and Methods). The upper panels show the complete data sets of two independent experiments up to a concentration of 50 $\mu$M free tau. The mutants are indicated in the upper left corner. The lower panels focus on the low concentration range (up to 1 $\mu$M free tau) important for the first binding phase. The left panels show the group of mutants with intermediate stoichiometries (htau40$^{wt}$ = control, G272V, V337M, and R406W). The right panels show the mutants which differ from the wild type by exhibiting a significantly higher stoichiometry (P301L and ΔK280) or a lower stoichiometry (N279K).

Table 1: Parameters of Tau−Microtubule Binding[a]

| mutant | $K_d/\mu$M | $n$ | $p/\mu$M | class | location | exon | isoform ratio |
|---|---|---|---|---|---|---|---|
| htau40$^{wt}$ | 0.075 ± 0.048 | 0.20 ± 0.04 | 45 ± 4 | m | − | − | 3R ∼ 4R |
| G272V | 0.090 ± 0.021 | 0.27 ± 0.04 | 52 ± 10 | m | R1 | 9 | 3R ∼ 4R |
| *N279K* | *0.006* ± 0.006 | *0.07* ± 0.02 | *25* ± 2 | *l* | R2 | 10 | mostly 4R |
| **ΔK280** | **0.135 ± 0.055** | **0.40 ± 0.07** | **52 ± 6** | **h** | R2 | 10 | mostly 3R |
| **P301L** | **0.063 ± 0.041** | **0.37 ± 0.09** | **53 ± 12** | **h** | R2 | 10 | 3R ∼ 4R |
| V337M | 0.032 ± 0.011 | 0.27 ± 0.02 | 38 ± 2 | m | R4 | 12 | 3R ∼ 4R |
| R406W | 0.090 ± 0.027 | 0.30 ± 0.05 | 44 ± 5 | m | CT | 13 | 3R ∼ 4R |

[a] Mutants of htau40 are listed in ascending order. The dissociation constant $K_d$, stoichiometry $n$, and overloading parameter $p$ (reminiscent of a second phase dissociation constant) were derived as described (*47*). The mutants were classified according to their stoichiometry of the first (high-affinity) binding phase: high (boldface type), medium, and low (italic type).

tendency to aggregate into PHFs or related structures. The aggregation was induced by heparin and quantitated with the thioflavine S fluorescence assay (*41*). While htau40$^{wt}$ aggregates very slowly over the course of ∼2 weeks, the mutants aggregate much faster (Figure 5). One group comprising G272V, N279K, V337M, and R406W shows a shorter half-time of 2.5−3 days and a final extent 1.5−2-fold higher than htau40$^{wt}$. Particularly remarkable is the rapid and extensive aggregation of ΔK280 (half-time 3.5 h, extent 5-fold over wild-type tau) and P301L (half-time 1.5 days, extent 3-fold over wild type). These parameters correlate well with the stoichiometry of microtubule binding (Figure 3) and suggest that the mutants possess some structural features that affect microtubule binding and PHF aggregation in a similar way; presumably, these elements reside in the repeat domain of tau because this is essential for microtubule interaction as well as PHF formation.

To test this assumption, we generated the mutations in the construct K18 which comprises the 4 repeats only (Figure 1), with the exception of R406W because this residue lies outside the repeat domain. In addition, we generated a double mutant, ΔK280/V337M, to see whether mutations had additive effects. Generally, shorter constructs of tau, lacking the C- and N-termini but containing the repeat region, assemble much faster into PHFs (*26*, *50*). This is also observed with the K18 mutants. As in the case of htau40, we can subdivide the mutants in groups of similar behavior (Figure 6). K18 itself and the mutants G272V and V337M belong in one group, with half-times around 4−5.5 h and similar extents of aggregation. In contrast to full-length tau, there is no major difference between K18$^{wt}$ and this group of mutants. This implies that the assembly inhibition by the domains flanking the repeats in full-length tau can be overcome either by a mutation in the repeats (see Figure 5) or by omitting the flanking domains (as in K18, Figure 6). Independently of that, the K18 mutants ΔK280 and P301L fall into a separate group because of their exceptionally fast aggregation (half-times of around 20 min and 2.5 h,

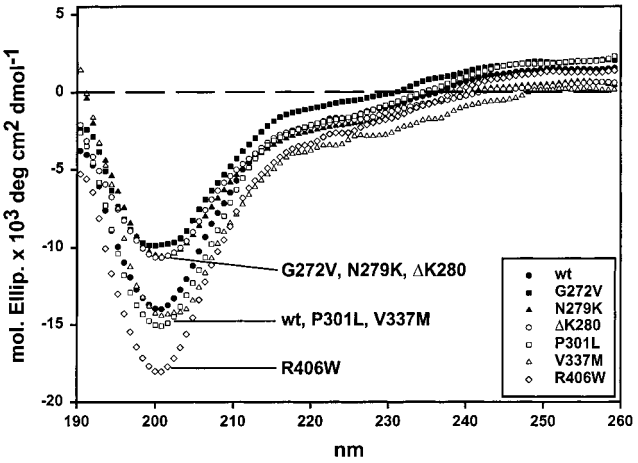


FIGURE 4: CD spectroscopy of htau40 mutants. CD spectra (molar ellipticities) were obtained at 20 $\mu$M protein concentrations in 10 mM ammonium acetate at room temperature. All curves show a pronounced minimum around 200 nm, indicative of a largely random coil structure. The minimum is deepest for R406W, is shallowest for G272V, N279K, and ΔK280, and has intermediate values for htau40$^{wt}$, P301L, and V337M.

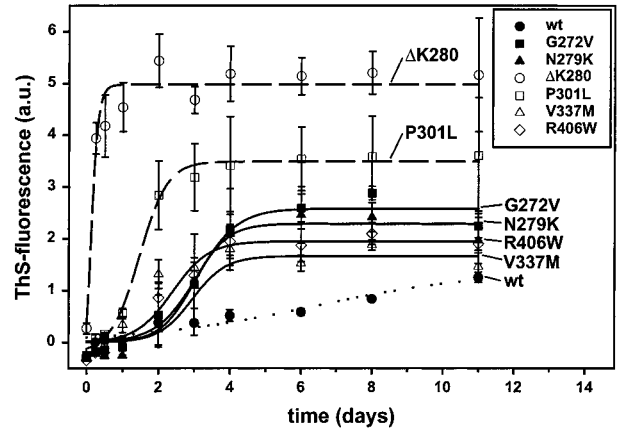


FIGURE 5: Aggregation of htau40 mutants into paired helical filaments. The kinetics of aggregation of htau40 mutants into PHFs were measured fluorometrically using the dye ThS (*29*). Tau protein concentrations were 50 $\mu$M and heparin concentration 12.5 $\mu$M in PBS, pH 7.4, containing 1 mM DTT. Prior to the addition of heparin and incubation at 37 °C, the samples were heated for 5 min at 50 °C to ensure complete reduction of tau to monomers. Shown is the average value ($n = 3$) with the standard deviation. Wild-type htau40 shows the slowest aggregation (dotted line); even after 11 days only a small fraction is converted to PHFs. The mutants generally aggregate more efficiently and can be divided into two groups: one of intermediate efficiency (G272V, N279K, V337M, and R406W, half times of 2.5−3 days and a final extent 1.5−2-fold higher than wild-type htau40) and one of high efficiency (ΔK280, half-time 3.5 h, and P301L, half-time ∼1.5 days; extent ∼3−5-fold higher).

respectively). The same behavior is seen with the double mutant ΔK280/V337M; this proves that the "fast" mutant ΔK280 overrides the "slow" mutant V337M and serves as a control for the reproducibility of the experiments (since the single and double mutants were generated and tested independently). As in the case of htau40, the P301L mutant of K18 polymerizes into filaments to a higher extent (1.5-fold higher). Note that in the case of K18 the two mutants ΔK280 and N279K (deletion or addition of a positive charge) have opposite effects.

*(e) Electron Microscopy of Tau Filaments.* To verify that the aggregation observed by the thioflavine S fluorescence assay resulted in filaments resembling PHFs, we investigated

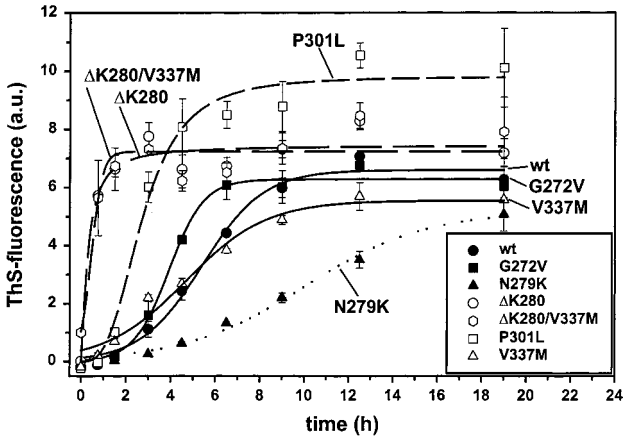


FIGURE 6: Aggregation of K18 mutants into paired helical filaments. The kinetics of aggregation of K18 mutants are observed by the ThS fluorescence assay. Conditions were similar as in Figure 5, except that the concentration of protein was 15 $\mu$M, heparin 3.8 $\mu$M, and DTT 10 mM. Shown is the average value ($n = 3$) with the standard deviation. In general, K18 aggregates much faster than full-length tau, with a half-time of ∼5.5 h (note the time scale in hours, not days). As for the htau40 mutants, the K18 mutants ΔK280 and P301L polymerize much faster and to a higher extent into PHFs than the wild type. The double mutant ΔK280−V337M shows the same characteristics as ΔK280 (dashed lines). K18 mutants G272V and V337M aggregate into filaments approximately with the same velocity (half-times 4−5.5 h) and to a similar extent as K18$^{wt}$ (solid lines). A slower aggregation (half-time 11 h) was observed for the mutant N279K (dotted line).

them by negative stain electron microscopy, using the same preparations (Figure 7). Aggregated htau40$^{wt}$ and its mutants G272V, ΔK280, and P301L showed filaments with the typical paired helical structure resembling Alzheimer PHFs as well as straight filaments. By contrast, mutants N279K, V337M, and R406W assembled mostly into straight filaments. In the case of the 4-repeat construct K18 and its mutants G272V, N279K, ΔK280, and V337M, we observed mostly a paired helical structure, with P301L straight filaments were also frequent. This suggests that the aggregation was based on similar structural principles in all cases.

## DISCUSSION

We investigated the effect of several tau mutants reported for FTDP-17, i.e., the missense mutations G272V (*10*), N279K (*11*), P301L (*12*), V337M (*12*), and R406W (*10*); and the deletion mutant ΔK280 (*14*). They all lie in the C-terminal microtubule-binding half of tau, mostly in the repeat domain (except R406W in the C-terminal tail, see Figure 1). Three of them (N279K, ΔK280, P301L) are in the second repeat coded by exon 10 (residues V275−S305) and therefore occur only in 4-repeat tau isoforms but not in 3-repeat forms lacking repeat 2. These mutants were cloned into the largest tau isoform of human CNS, htau40, and expressed in *E. coli*. In addition we generated the same mutants on the basis of the 4-repeat construct K18 (except R406W) because tau constructs comprising the repeats aggregate into PHFs more readily than full-length tau (*26*). The mutants were tested for their capability to promote microtubule assembly, binding to microtubules (preformed and stabilized with taxol), secondary structure as seen by circular dichroism, PHF assembly in solution (by the ThS fluorescence assay), and filament structure by electron microscopy.

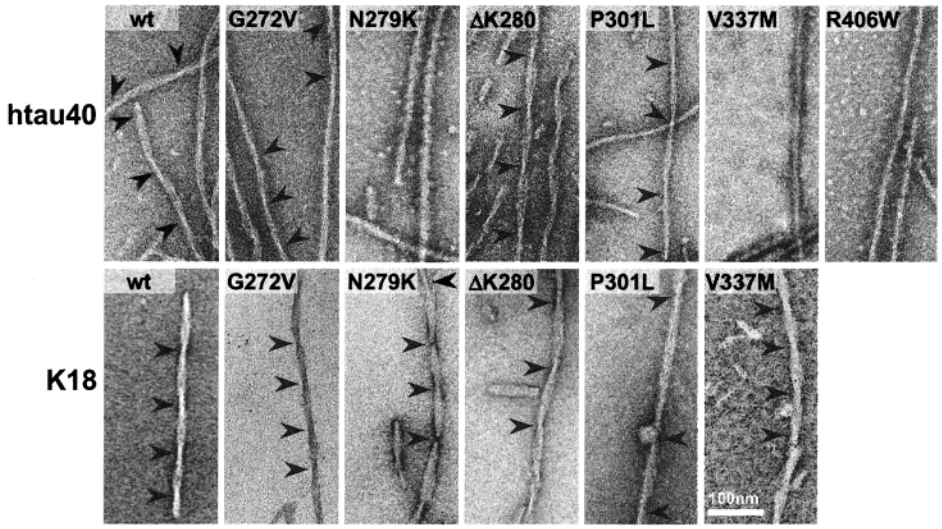


FIGURE 7: Negative stain electron microscopy of filaments of tau mutants. Filaments of htau40 and its mutants (upper panel) and K18 mutants (lower panel) assembled in the presence of heparin (same filament preparations as for the kinetic data at the endpoint of assembly). Bar = 100 nm. *htau40:* wild type, G272V, ΔK280, and P301L showed filaments with the typical paired helical structure as well as straight filaments. In contrast, N279K, V337M, and R406W formed predominantly straight filaments. *K18:* wild type, G272V, N279K, ΔK280, and V337M showed mostly paired helical structure whereas P301L formed largely straight filaments.

The mechanism of action of these mutants in the disease is currently not understood. The two major features of tau in degenerating neurons are their detachment from microtubules (which become less stable), and their aggregation into PHFs. It is therefore tempting to speculate that mutants cause the disease by binding less tightly to microtubules or by aggregating into PHFs more readily. However, these issues are complicated by the fact that tau mutations also cause a shift in the isoform expression pattern, compared to the normal situation where 3R and 4R isoforms are present in roughly equal amounts. For example, 4R-tau isoforms become dominant in the case of the mutations N279K, L284L, and S305N and the intronic mutations that are silent on the protein level because exon 10 is preferentially spliced in (*10*, *11*, *17*, *18*, *31*, *34*, *51*). 3R-tau is dominant in the case of ΔK280 because an exon splicing enhancer element is disrupted (*15*), but no major changes in isoform expression are observed for the mutants G272V, P301L, V337M, and R406W. Since 4R isoforms generally bind and stimulate microtubules better than 3R forms, the shift to 4R forms could override any mutation that might weaken the binding. Superimposed on this issue is the question of overall tau expression; if this were enhanced, it could overstabilize microtubules (and thus limit their dynamic instability), regardless of mutations. It has been reported that tau is generally elevated in Alzheimer's disease (*52*). Alternatively, the disease-causing mechanism could lie in some other property of tau protein or tau mRNA. For example, elevated tau causes an inhibition of the transport of vesicles and organelles toward the synapse (*53*), and tau serves as an anchor for phosphatases and regulates their activity (*54*, *55*). This might explain why the severity of the disease does not correlate well with the known biochemical parameters of tau (*56*, *57*). As a case in point, mutations in the microtubule-dependent motor protein kinesin have different effects in the fruit fly *Drosophila*, but these are not necessarily related to the functioning of the motor domain as such; one functionally minor mutation is lethal because the protein is not expressed properly (*58*). Finally, mutations in tau cause disease in an autosomal dominant fashion. This implies that mutant tau derived from one allele must acquire an additional (toxic) function which becomes visible even in the presence of the wild-type tau derived from the other allele.

The difficulties in interpreting functional differences are highlighted by our findings. They can be summarized as follows:

*(1) Microtubule Assembly.* All tau mutants stimulate microtubule assembly to a somewhat lesser degree than htau$^{wt}$ (Figure 2). This could be used to argue that microtubule stabilization is impaired in the disease. In our hands, ΔK280 or R406W reproducibly show the weakest effect, P301L the strongest. This gradient agrees with that of Hasegawa et al. (*33*, *34*) and differs from that of Hong et al. (*31*), but since the change is not large it is not clear how significant it is. Overall, the effects are moderate, and the differences between the mutants are not pronounced, consistent with results of others (e.g., *15*, *33*). In the case of N279K, one would expect that the loss of microtubule stabilization is more than compensated by the increase in 4R isoforms; conversely, ΔK280 would reduce microtubule stability mainly by reducing 4R isoforms in favor of 3R isoforms.

*(2) Microtubule Binding.* This behavior shows wide variations, but is also the most difficult to assess since it cannot be described by a simple monophasic approach to equilibrium (Figure 3) (*47*). This is in contrast to the usual interpretation, and therefore our values are not directly comparable with those of others. The stoichiometry of the tight binding phase can serve as a basis for classification into three groups (Table 1): an intermediate group (htau40$^{wt}$, G272V, V337M, R406W) with $n \sim 0.2-0.3$, first-phase $K_d < 0.1$ $\mu$M, and $p \sim 40-50$ $\mu$M; a high binding group (ΔK280 and P301L) with $n \sim 0.4$ but little change in the other parameters; and the low binding group of N279K with $n \sim 0.07$ and a low $p$-value so that binding becomes noticeable only at high concentrations. Independently of tau's capacity to promote microtubule assembly, the binding to microtubules could influence other parameters such as the anchoring of enzymes, spacing between microtubules and other cell components, and the regulation of intracellular

organelle transport. However, given that the mutant tau molecules function in a background of normal tau, the observed changes in binding behavior do not appear substantial enough to explain pathological consequences.

*(3) Secondary Structure.* All tau isoforms are dominated by a random coil structure in solution *(48)*, and this holds for the mutants as well (Figure 4; see also *37*). In the CD spectra, this leads to a characteristic trough at 200 nm. The depth of the trough is variable (between −10 and −18 in Figure 4), lowest for R406W, intermediate for the group of htau40$^{wt}$, V337M, and P301L, and shallowest for the group of G272V, N279K, and ΔK280. However, in the case of largely random structures such as tau, these differences do not lend themselves to a more detailed interpretation, and therefore it is not possible to conclude that the mutations cause extended conformational changes. In contrast to others (*59*), we found no evidence for a pronounced shift toward α-helical structure. There is also no obvious correlation betweeen the CD spectra and the microtubule assembly stimulation by the mutants (Figure 2). We conclude that if structural changes occur, they must be of a local nature, not visible by CD spectroscopy.

*(4) PHF Aggregation.* It is remarkable that all mutants tested aggregate more readily than htau40$^{wt}$ (Figure 5). The group G272V, N279K, V337M, and R406W shows a comparable intermediate enhancement, whereas the group of ΔK280 and P301L aggregate unusually fast. The enhancement of aggregation by P301L is broadly consistent with the observations of other authors based on electron microscopy and other methods (*37*−*40*). The speed of aggregation becomes further accentuated when the inhibitory domains of the N-terminus and the C-terminus are removed, as in the 4-repeat construct K18 (Figure 6). In this case, K18$^{wt}$ and the mutants G272V and V337M show roughly similar rates and extents of aggregation. This illustrates that PHF aggregation is normally retarded by the domains outside the repeats (especially the N-terminal half), but that this inhibition can be compensated by a single point mutation in the repeat domain. As in the case of full-length tau, the mutations P301L and ΔK280 cause an exceptionally rapid aggregation. This change in behavior represents a toxic gain of function which would be noticeable even in the presence of normal tau. Moreover, since PHF assembly is a nucleation-dependent process (*29*), nuclei formed by mutant tau could be elongated even from the pool of normal tau and thus poison the entire tau population in a cell.

In summary, the known missense and deletion mutants of tau found in FTDP-17 dementias clearly change the biochemical behavior of the protein in vitro. This is exemplified by a somewhat reduced capacity to induce the assembly of microtubules, and by an enhanced capacity to aggregate into paired helical filaments similar to those of FTDP-17, Alzheimer's disease, and related tauopathies. This latter property would be consistent with a toxic gain of function that would be expected from the autosomal dominant nature of the FTDP-17 tauopathies. We have recently described a short hexapeptide sequence ($^{306}$VQIVYK$^{311}$) in the third repeat and a similar motif ($^{275}$VQIINK$^{280}$) in the second repeat, whose local transformation to β-structure (within a global random-coil structure) is important for PHF aggregation (*50*). A similar mechanism applies to the aggregation of tau mutants which also show increased β-structure upon aggregation (data not shown). Thus, while some of the FTDP-17 mutations in the tau gene appear to operate by changing the pattern of alternative splicing on the mRNA level, others could possibly influence the propensity for β-structure on the protein level. This question is currently under investigation.

## ACKNOWLEDGMENT

We are grateful to Winfried Beyer, Anja Konopatzki, Nathalie Habbe, Karin Blume, and Brigitte Krüger for help during the generation of the mutant tau clones and the preparation of the protein.

## REFERENCES

1. Johnson, G. V. W., and Hartigan, J. A. (1998) *Alzheimer's Dis. Rev. 3*, 125−141.
2. Mandelkow, E. M., and Mandelkow, E. (1998) *Trends Cell Biol. 8*, 425−427.
3. Braak, H., and Braak, E. (1991) *Acta Neuropathol. 82*, 239−259.
4. Arriagada, P. V., Growdon, J. H., Hedley-Whyte, E., and Hyman, B. T. (1992) *Neurology 42*, 631−639.
5. Terry, R. D. (1996) *J. Neuropathol. Exp. Neurol. 55*, 1023−1025.
6. Spillantini, M. G., and Goedert, M. (1998) *Trends Neurosci. 21*, 428−433.
7. Wilhelmsen, K. C. (1999) *Proc. Natl. Acad. Sci. U.S.A. 96*, 7120−7121.
8. Selkoe, D. J. (1998) *Trends Cell Biol. 8*, 447−453.
9. Foster, N. L., Wilhelmsen, K., Sima, A. A., Jones, M. Z., D'Amato, C. J., and Gilman, S. (1997) *Ann. Neurol. 41*, 706−715.
10. Hutton, M., Lendon, C. L., Rizzu, P., Baker, M., Froelich, S., Houlden, H., Pickering-Brown, S., Chakraverty, S., Isaacs, A., Grover, A., Hackett, J., Adamson, J., Lincoln, S., Dickson, D., Davies, P., Petersen, R. C., Stevens, M., de Graaff, E., Wauters, E., van Baren, J., Hillebrand, M., Joosse, M., Kwon, J. M., Nowotny, P., Heutink, P., and et al. (1998) *Nature 393*, 702−705.
11. Clark, L. N., Poorkaj, P., Wszolek, Z., Geschwind, D. H., Nasreddine, Z. S., Miller, B., Li, D., Payami, H., Awert, F., Markopoulou, K., Andreadis, A., I, D. S., Lee, V. M., Reed, L., Trojanowski, J. Q., Zhukareva, V., Bird, T., Schellenberg, G., and Wilhelmsen, K. C. (1998) *Am. J. Pathol. 153*, 1359−1363.
12. Poorkaj, P., Bird, T. D., Wijsman, E., Nemens, E., Garruto, R. M., Anderson, L., Andreadis, A., Wiederholt, W. C., Raskind, M., and Schellenberg, G. D. (1998) *Ann. Neurol. 43*, 815−825.
13. Iijima, M., Tabira, T., Poorkaj, P., Schellenberg, G. D., Trojanowski, J. Q., Lee, V. M., Schmidt, M. L., Takahashi, K., Nabika, T., Matsumoto, T., Yamashita, Y., Yoshioka, S., and Ishino, H. (1999) *Neuroreport 10*, 497−501.
14. Rizzu, P., Van Swieten, J. C., Joosse, M., Hasegawa, M., Stevens, M., Tibben, A., Niermeijer, M. F., Hillebrand, M., Ravid, R., Oostra, B. A., Goedert, M., van Duijn, C. M., and Heutink, P. (1999) *Am. J. Hum. Genet. 64*, 414−421.
15. D'Souza, D. I., Poorkaj, P., Hong, M., Nochlin, D., Lee, V. M., Bird, T. D., Schellenberg, G. D., Arawaka, S., Usami, M., Sahara, N., Schellenberg, G. D., Lee, G., and Mori, H. (1999) *Proc. Natl. Acad. Sci. U.S.A. 96*, 5598−5603.
16. Spillantini, M. G., Murrell, J. R., Goedert, M., Farlow, M. R., Klug, A., and Ghetti, B. (1998) *Proc. Natl. Acad. Sci. U.S.A. 95*, 7737−7741.
17. Varani, L., Hasegawa, M., Spillantini, M. G., Smith, M. J., Murrell, J. R., Ghetti, B., Klug, A., Goedert, M., and Varani, G. (1999) *Proc. Natl. Acad. Sci. U.S.A. 96*, 8229−8234.
18. Grover, A., Houlden, H., Baker, M., Adamson, J., Lewis, J., Prihar, G., Pickering-Brown, S., Duff, K., and Hutton, M. (1999) *J. Biol. Chem. 274*, 15134−15143.

19. Butner, K. A., and Kirschner, M. W. (1991) *J. Cell Biol. 115*, 717−730.
20. Gustke, N., Trinczek, B., Biernat, J., Mandelkow, E. M., and Mandelkow, E. (1994) *Biochemistry 33*, 9511−9522.
21. Goode, B. L., Denis, P. E., Panda, D., Radeke, M. J., Miller, H. P., Wilson, L., and Feinstein, S. C. (1997) *Mol. Biol. Cell 8*, 353−365.
22. Panda, D., Miller, H. P., and Wilson, L. (1999) *Proc. Natl. Acad. Sci. U.S.A. 96*, 12459−12464.
23. Jordan, M. A., and Wilson, L. (1998) *Curr. Opin. Cell Biol. 10*, 123−130.
24. Wischik, C., Novak, M., Thogersen, H., Edwards, P., Runswick, M., Jakes, R., Walker, J., Milstein, C., Roth, M., and Klug, A. (1988) *Proc. Natl. Acad. Sci. U.S.A. 85*, 4506−4510.
25. Novak, M., Kabat, J., and Wischik, C. M. (1993) *EMBO J. 12*, 365−370.
26. Wille, H., Drewes, G., Biernat, J., Mandelkow, E. M., and Mandelkow, E. (1992) *J. Cell Biol. 118*, 573−584.
27. Perez, M., Valpuesta, J. M., Medina, M., Degarcini, E. M., and Avila, J. (1996) *J. Neurochem. 67*, 1183−1190.
28. Hasegawa, M., Crowther, R. A., Jakes, R., and Goedert, M. (1997) *J. Biol. Chem. 272*, 33118−33124.
29. Friedhoff, P., von Bergen, M., Mandelkow, E. M., Davies, P., and Mandelkow, E. (1998) *Proc. Natl. Acad. Sci. U.S.A. 95*, 15712−15717.
30. King, M. E., Gamblin, T. C., Kuret, J., and Binder, L. I. (2000) *J. Neurochem. 74*, 1749−1757.
31. Hong, M., Zhukareva, V., Vogelsberg-Ragaglia, V., Wszolek, Z., Reed, L., Miller, B. I., Geschwind, D. H., Bird, T. D., McKeel, D., Goate, A., Morris, J. C., Wilhelmsen, K. C., Schellenberg, G. D., Trojanowski, J. Q., and Lee, V. M. (1998) *Science 282*, 1914−1917.
32. DeTure, M., Ko, L., Yen, S., Nacharaju, P., Easson, C., Lewis, J., van Slegtenhorst, M., and Hutton, M. (2000) *Brain Res. 853*, 5−14.
33. Hasegawa, M., Smith, M. J., and Goedert, M. (1998) *FEBS Lett. 437*, 207−210.
34. Hasegawa, M., Smith, M. J., Iijima, M., Tabira, T., and Goedert, M. (1999) *FEBS Lett. 443*, 93−96.
35. Dayanandan, R., Van Slegtenhorst, M., Mack, T. G., Ko, L., Yen, S. H., Leroy, K., Brion, J. P., Anderton, B. H., Hutton, M., and Lovestone, S. (1999) *FEBS Lett. 446*, 228−232.
36. Matsumura, N., Yamazaki, T., and Ihara, Y. (1999) *Am. J. Pathol. 154*, 1649−1656.
37. Goedert, M., Jakes, R., and Crowther, R. A. (1999) *FEBS Lett. 450*, 306−311.
38. Arrasate, M., Perez, M., Armas-Portela, R., and Avila, J. (1999) *FEBS Lett. 446*, 199−202.
39. Nacharaju, P., Lewis, J., Easson, C., Yen, S., Hackett, J., Hutton, M., and Yen, S. H. (1999) *FEBS Lett. 447*, 195−199.
40. Gamblin, T. C., King, M. E., Dawson, H., Vitek, M. P., Kuret, J., Berry, R. W., and Binder, L. I. (2000) *Biochemistry 39*, 6136−6144.
41. Friedhoff, P., Schneider, A., Mandelkow, E. M., and Mandelkow, E. (1998) *Biochemistry 37*, 10223−10230.
42. Biernat, J., Mandelkow, E. M., Schröter, C., Lichtenberg-Kraag, B., Steiner, B., Berling, B., Meyer, H. E., Mercken, M., Vandermeeren, A., Goedert, M., and Mandelkow, E. (1992) *EMBO J. 11*, 1593−1597.
43. Goedert, M., Wischik, C., Crowther, R., Walker, J., and Klug, A. (1988) *Proc. Natl. Acad. Sci. U.S.A. 85*, 4051−4055.
44. Greenfield, N., and Fasman, G. D. (1969) *Biochemistry 8*, 4108−4116.
45. Deleage, G., Blanchet, C., and Geourjon, C. (1997) *Biochimie 79*, 681−686.
46. Gaskin, F., Cantor, C. R., and Shelanski, M. L. (1974) *J. Mol. Biol. 89*, 737−755.
47. Ackmann, M., Wiech, H., and Mandelkow, E. (2000) *J. Biol. Chem.* (in press).
48. Schweers, O., Schönbrunn-Hanebeck, E., Marx, A., and Mandelkow, E. (1994) *J. Biol. Chem. 269*, 24290−24297.
49. Chou, P. Y., and Fasman, G. D. (1978) *Annu. Rev. Biochem. 47*, 251−276.
50. von Bergen, M., Friedhoff, P., Biernat, J., Heberle, J., and Mandelkow, E. (2000) *Proc. Natl. Acad. Sci. U.S.A. 97*, 5129−5134.
51. Gao, Q. S., Memmott, J., Lafyatis, R., Stamm, S., Screaton, G., and Andreadis, A. (2000) *J. Neurochem. 74*, 490−500.
52. Khatoon, S., Grundke-Iqbal, I., and Iqbal, K. (1992) *J. Neurochem. 59*, 750−753.
53. Ebneth, A., Godemann, R., Stamer, K., Illenberger, S., Trinczek, B., and Mandelkow, E. (1998) *J. Cell Biol. 143*, 777−794.
54. Liao, H., Li, Y., Brautigan, D. L., and Gundersen, G. G. (1998) *J. Biol. Chem. 273*, 21901−21908.
55. Sontag, E., Nunbhakdi-Craig, V., Lee, G., Brandt, R., Kamibayashi, C., Kuret, J., White, C. L., 3rd, Mumby, M. C., and Bloom, G. S. (1999) *J. Biol. Chem. 274*, 25490−25498.
56. Bird, T. D., Nochlin, D., Poorkaj, P., Cherrier, M., Kaye, J., Payami, H., Peskind, E., Lampe, T. H., Nemens, E., Boyer, P. J., and Schellenberg, G. D. (1999) *Brain 122*, 741−756.
57. van Swieten, J. C., Stevens, M., Rosso, S. M., Rizzu, P., Joosse, M., de Koning, I., Kamphorst, W., Ravid, R., Spillantini, M. G., Niermeijer, and Heutink, P. (1999) *Ann. Neurol. 46*, 617−626.
58. Brendza, K. M., Rose, D. J., Gilbert, S. P., and Saxton, W. M. (1999) *J. Biol. Chem. 274*, 31506−31514.
59. Jicha, G. A., Rockwood, J. M., Berenfeld, B., Hutton, M., and Davies, P. (1999) *Neurosci. Lett. 260*, 153−156.

BI000850R